

Sugars to Control Ligand Shape in Metal Complexes: Conformationally Constrained Glycoligands with a Predetermination of Stereochemistry and a Structural Control

Ludivine Garcia,[†] Stéphane Maisonneuve,[§] Juan Xie,[§] Régis Guillot,[‡] Pierre Dorlet,^{||} Eric Rivière,[‡] Michel Desmadril,[⊥] François Lambert,^{†,‡} and Clotilde Policar^{*,†,‡}

[†]Laboratoire des Biomolécules, UMR7203, Département Chimie de l'ENS, Université Pierre et Marie Curie, 24 rue Lhomond F-75231 Paris Cedex 05 France, [‡]Institut de Chimie Moléculaire et des Matériaux d'Orsay, Université Paris-Sud 11, F-91405 Orsay Cedex France, [§]PPSM, Institut d'Alembert, ENS Cachan, CNRS, 61 av Prsd Wilson, F-94230 Cachan, France, ^{||}CNRS, URA 2096, Laboratoire du Stress Oxydant et Détoxication, iBiTec-S CEA Saclay, F-91191 Gif-sur-Yvette, France, and [⊥]Institut de Biochimie et Biophysique Moléculaire et Cellulaire (UMR8619), Université Paris-Sud 11 F-91405 Orsay Cedex, France

Received February 5, 2010

In coordination chemistry, ligand shape can be used to tune properties, such as metal selectivity, coordination number, electronic structure, redox potential, and metal center stereochemistry including coordination helicates formation, and also to generate cavities for encapsulation. The results presented in this article indicate that two epimeric glycoligands (**3** and **4**) based on the conformationally restrained *xyl*- and *ribo*-1,2-*O*-isopropylidene-furano scaffolds are preorganized in water through π – π stacking due to hydrophobic interactions, as evidenced from excimer observation. The structure obtained in the solid state for one of the Cu(II) complexes (**5**) is chiral, with an original helical chirality arising from the coiling of the two ligands around the Cu–Cu axis. It shows an unusual double-deck type structure, with π – π interaction between two triazolyl-pyridyl rings and with a small cavity between the two Cu(II) ions able to host a bridging water molecule, as suggested by electron paramagnetic resonance. The Cu(II) complex from the epimeric ligand (**6**) shows similar properties with a mirror-image CD spectrum in the d–d region of the Cu(II). There is a predetermination of chirality at the metal center by the glycoligand induced by the C3 configuration, **6** and **5** being pseudoenantiomers. Interestingly, the stereochemistry at the metal center is here controlled by the combination of π -stacking and chiral backbone.

Introduction

In coordination chemistry, ligand shape can be used to tune properties, such as coordination number,¹ electronic structure, redox potential,² and metal center stereochemistry including coordination helicates formation,³ and also to generate cavities for encapsulation.⁴ To control the shape,

conformationally constrained ligands, such as ligands bearing bulky substituents,⁵ substituted macrocycles,⁶ capped calixarenes,⁷ and nonmacrocylic ligands,⁸ have been developed in the literature. However, and although monosaccharides have been extensively used in organic synthesis as valuable platforms to tailor molecular diversity,⁹ their involvement as conformationally constrained central structures in coordination chemistry is still scarce. Except in a few examples,¹⁰ sugars are used as appended moieties to design ligands and complexes for asymmetric catalysis^{11–13} or biomedical applications.^{14,15}

*Corresponding author. Fax: (+) 33-101 44 32 33 97. E-mail: clotilde.policar@ens.fr.

(1) Lee, K.; Matzapetakis, M.; Mitra, S.; Marsh, E.; Pecoraro, V. *J. Am. Chem. Soc.* **2004**, *126*, 9178–9179.

(2) Comba, P. *Coord. Chem. Rev.* **2009**, *253*, 564–574.

(3) He, C.; Zhao, Y.; Guo, D.; Lin, Z.; Duan, C. *Eur. J. Inorg. Chem.* **2007**, 3451–3463.

(4) Fiedler, D.; Leung, D. H.; Bergman, R. G.; Raymond, K. N. *Acc. Chem. Res.* **2005**, *38*, 351–360.

(5) Jiang, X.; Bollinger, J. C.; Lee, D. *J. Am. Chem. Soc.* **2005**, *127*, 15678–15679.

(6) Hubin, T. *J. Coord. Chem. Rev.* **2003**, *241*, 27–46.

(7) Zeng, X.; Coquière, D.; Alenda, A.; Prangé, T.; Li, Y.; Reinaud, O.; Jabin, I. *Chem.—Eur. J.* **2006**, *12*, 6393–6402.

(8) Hancock, R. D.; Melton, D. L.; Harrington, J. M.; McDonald, F. C.; Gephart, R. T.; Boone, L. L.; Jones, S. B.; Dean, N. E.; Whitehead, J. R.; Cockrell, G. M. *Coord. Chem. Rev.* **2007**, *251*, 1678–1689.

(9) Gruner, S. A. W.; Locardi, E.; Lohof, E.; Kessler, H. *Chem. Rev.* **2002**, *102*, 491–514.

(10) Dhungana, S.; Harrington, J. M.; Gebhardt, P.; Moellmann, U.; Crumbliss, A. L. *Inorg. Chem.* **2007**, *45*, 8362–8371.

(11) Diéguez, M.; Pàmies, O.; Ruiz, A.; Diaz, Y.; Castillon, S.; Claver, C. *Coord. Chem. Rev.* **2004**, *248*, 2165–2192.

(12) Wegner, R.; Gottschaldt, M.; Görls, H. *Angew. Chem., Int. Ed.* **2000**, *39*, 595–599.

(13) Totani, K.; Takao, K.; Tadano, K. *Synlett* **2004**, *12*, 2066–2080.

(14) Storr, T.; Merkel, M.; Song-Zhao, G. X.; Scott, L. E.; Green, D. E.; Bowen, M. L.; Thompson, K. H.; Patrick, B. O.; Schugar, H. J.; Orvig, C. *J. Am. Chem. Soc.* **2007**, *129*, 7453–7463.

(15) Gottschaldt, M.; Schubert, U. *Chem.—Eur. J.* **2009**, *15*, 1548–1557.

We have recently introduced a strategy that uses sugars as central platforms to generate tunable chelation sites for transition-metal cations.^{16,17} In these glycoligands,^{18–22} the conformational rigidity of the sugar platform is of interest to induce a structural control of the chelation site. Here, a pair of epimeric bicyclic pentofuranoses was used to generate ligands by appending bidentate pyrid-2'-yl-1,2,3-triazole. These central furanose backbones are conformationally constrained bicyclic *xylo-* or *ribo-*1,2-*O*-isopropylidene-furano scaffolds.^{23,24} The pyrid-2'-yl-1,2,3-triazole claw has been chosen for its rigidity and planarity, with possible interaction through π -stacking. Interestingly, a dimeric Cu(II) double-deck complex has been crystallized with one of the ligands, and the structure showed an helical chirality and a small cavity between the two Cu(II)-ions. The two complexes derived from the two epimeric ligands were shown to be pseudoenantiomers. The following study emphasizes the effect of the central scaffold and π -stacking on the structural properties of the complexes.

Experimental Section

Materials and Methods. All reagents employed (high-grade purity materials) were commercially available and used as supplied (Aldrich and Acros Organics). Chromatography was carried out using silica gel 60 Å (330–400 mesh). For thin-layer chromatography (TLC), Merck silica gel 60 Å (layer: 0.20 mm) with fluorescent indicator UV₂₅₄ on aluminum sheets was used. Infrared spectra were recorded on a Bruker IFS 66 FT-IR spectrometer in the range 4000–400 cm⁻¹. Electronic spectra of the copper complexes were recorded on a Cary-300-Bio spectrophotometer and carried out in aqueous solution at 20 °C. Electron paramagnetic resonance (EPR) spectra were recorded on an X-band Bruker Elexsys 500 spectrometer equipped with a continuous flow helium cryostat (Oxford Instruments). The spectra were all recorded under nonsaturating conditions. It should be noted that the complexes are not very soluble in organic conditions. A toluene/acetone/DMSO 3:3:4 solvent had to be used for which no precipitation was observed. This is not a classical mixture to provide a good EPR-glass, which can explain the broad features observed experimentally for the EPR spectra in organic solvent. Cyclic voltammetry data were collected under argon atmosphere, using an Autolab potentiostat. The complexes (10⁻³ mol L⁻¹) were dissolved in water containing KNO₃ (0.2 mol L⁻¹). Glassy carbon was used as a working electrode, and platinum wire and ECS were used as auxiliary and reference electrode, respectively. Circular dichroism (CD) measurements were carried out on a JASCO J-170 spectropolarimeter (Xe-lamp) at 20 °C with optical-grade solvents and quartz glass cuvettes with a 10 mm path length. Elemental analyses were performed at the Centre National de

la Recherche Scientifique (CNRS, Gif-sur-Yvette). Nuclear magnetic resonance (NMR) spectra were obtained from dilute solutions in CDCl₃ at approximately 25 °C and recorded on Bruker DRX 300 (¹H, 300.132 MHz; ¹³C, 75.475 MHz) and AV 360 spectrometers (¹H, 360.113 MHz; ¹³C, 90.559 MHz). The residual solvent signals were used as internal standards: CDCl₃ (¹H δ = 7.27 ppm, ¹³C δ = 77.0 ppm). The resonance multiplicity is indicated as s (singlet), d (doublet), t (triplet), q (quartet), and m (multiplet). High-resolution electrospray spectra were recorded on a Finnigan MAT95S in a BE configuration. Fluorescence emission spectra were recorded on a Jobin-Yvon Spex Fluorolog 1681 spectrofluorimeter. The titration experiment was conducted in water:DMSO (85:15) solution. The fluorescence spectra were corrected from the O.D. at 260 nm by a multiplied factor of 1/1–10^{(-O.D.(260 nm))} and from the fluorescence spectra of the solvent. The evolution of the full fluorescence intensity from the ligands **3** and **4** as a function of Cu(II) concentration contains information on the stability constant of the complex through the following equation: $Y(C_M) = Y_0 + 0.5 \times (Y_{\text{lim}} - Y_0) \times [1 + C_M/C_L + 1/(K \times C_L) - [(1 + C_M/C_L + 1/(K \times C_L))^2 - 4 \times C_M/C_L]^{1/2}]$, where Y designates the fluorescence intensity of a C_L-concentrated solution (C_L = 8 × 10⁻⁶ mol L⁻¹) of ligand as a function of the concentration C_M of added cation. Y_0 and Y_{lim} are the fluorescence intensity values for C_M = 0 and for full complexation, respectively. K is the stability constant of the 1:1 complex.

General Procedure for the Synthesis of **3 and **4**.** Syntheses of **1** and **2** were previously published²⁵ but were presently prepared using other reported procedures.^{26–29} To a solution of **1**, (**2**) (500 mg, 1.9 mmol) in *t*-BuOH (5 mL) was added sodium ascorbate (263 mg, 1.3 mmol), copper(II) sulfate (160 mg, 0.7 mmol), and water (5 mL). After the change of color (white to purple), 2-ethynylpyridine (431 mg, 4.2 mmol) was added. The mixture was orange. After being stirred for one night at room temperature (r.t.), the green mixture was extracted with 3 × 10 mL of CH₂Cl₂. The organic phases were then washed with an aqueous solution of EDTA (0.1 mol L⁻¹) until the aqueous phase became colorless. The organic phase was dried over Na₂SO₄. After evaporation, the yellow solid obtained was purified on silica gel (CH₂Cl₂/EtOAc/MeOH 8.5:1.5:0.5) to afford a white powder in 91% yield (62%). The lower yield of **4** can be explained by a loss of product during the purification on the silica gel column.

3,5-Dideoxy-3,5-di(pyridin-2'-yl-1,2,3-triazol-1-yl)-1,2-O-isopropylidene- α -D-xylofuranose (3**).** R_f = 0.58 (DCM/EtOAc/MeOH 8.5:1:0.5); ¹H NMR (360 MHz, CDCl₃): δ = 8.57 (m, 2H, 2 × H_{Py}), 8.31 (s, 1H, H_{triazole}), 8.18 (dt, ³J(H,H) = 7.8 Hz, ⁴J(H,H) = 1.5 Hz, 1H, H_{Py}), 8.17 (s, 1H, H_{triazole}), 8.13 (dt, ³J(H,H) = 7.8 Hz, ⁴J(H,H) = 1.8 Hz, 1H, H_{Py}), 7.78 (dt, ³J(H,H) = 7.8 Hz, ⁴J(H,H) = 1.5 Hz, 1H, H_{Py}), 7.75 (dt, ³J(H,H) = 7.8 Hz, ⁴J(H,H) = 1.8 Hz, 1H, H_{Py}), 7.24 (ddd, ³J(H,H) = 7.8 Hz, ⁴J(H,H) = 4.8 Hz, ⁵J(H,H) = 1.1 Hz, 1H, H_{Py}), 7.21 (ddd, ³J(H,H) = 7.8 Hz, ⁴J(H,H) = 4.8 Hz, ⁵J(H,H) = 1.1 Hz, 1H, H_{Py}), 6.35 (d, ³J(H,H) = 3.6 Hz, 1H, H1), 5.38 (d, ³J(H,H) = 3.7 Hz, 1H, H3), 5.07 (d, ³J(H,H) = 3.6 Hz, 1H, H2), 4.96 (ddd, ³J(H,H) = 7.1 Hz, ³J(H,H) = 5.4 Hz, ³J(H,H) = 3.7 Hz, 1H, H4), 4.34 (dd, ²J(H,H) = 14.5 Hz, ³J(H,H) = 5.4 Hz, 1H, H5'), 4.08 (dd, ²J(H,H) = 14.5 Hz, ³J(H,H) = 7.1 Hz, 1H, H5), 1.53 (s, 3H, CH₃), 1.36 (s, 3H, CH₃); ¹³C NMR (75 MHz, CDCl₃): δ = 149.9, 149.5, 149.4, 148.9, 148.6, 137.0, 136.9, 123.3, 123.2,

(25) Koth, D.; Fiedler, A.; Scholz, M.; Gottschaldt, M. *J. Carbohydr. Chem.* **2007**, *26*, 267–278.

(26) Saito, Y.; Zevaco, T. A.; Agrofoglio, L. A. *Tetrahedron* **2002**, *58*, 9593–9603.

(27) Vatele, J.; Hanessian, S. *Tetrahedron* **1996**, *52*, 10557–10568.

(28) Izquierdo, I.; Plaza, M. T.; Robles, R.; Rodriguez, C.; Ramirez, A.; Mota, A. *Eur. J. Org. Chem.* **1999**, 1269–1274.

(29) David, O.; Maisonneuve, S.; Xie, J. *Tetrahedron Lett.* **2007**, *48*, 6527–6530.

(16) Cisnetti, F.; Guillot, R.; Thérissod, M.; Policar, C. *Acta Crystallogr., Sect. C: Cryst. Struct. Commun.* **2007**, *C63*, m201–m203.

(17) Cisnetti, F.; Guillot, R.; Ibrahim, N.; Lambert, F.; Thérissod, M.; Policar, C. *Carbohydr. Res.* **2008**, *343*, 530–535.

(18) Cisnetti, F.; Guillot, R.; Thérissod, M.; Desmadril, M.; Policar, C. *Inorg. Chem.* **2008**, *47*, 2243–2245.

(19) Bellot, F.; Hardré, R.; Pelosi, G.; Thérissod, M.; Policar, C. *Chem. Commun.* **2005**, 5414–5417.

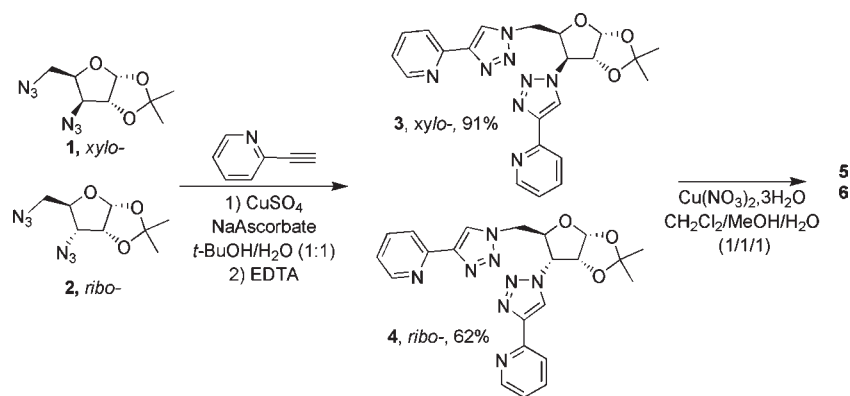
(20) Charron, G.; Bellot, F.; Cisnetti, F.; Pelosi, G.; Rebilly, J.; Rivière, E.; Barra, A.; Mallah, T.; Policar, C. *Chem.—Eur. J.* **2007**, *13*, 2774–2782.

(21) Damaj, Z.; Cisnetti, F.; Dupont, L.; Henon, E.; Policar, C.; Guillon, E. *Dalton Trans.* **2008**, 3235–3245.

(22) Cisnetti, F.; Guillot, R.; Desmadril, M.; Pelosi, G.; Policar, C. *Dalton Trans.* **2007**, 1473–1476.

(23) Houseknecht, J. B.; McCarren, P. R.; Lowary, T. L.; Hadad, C. M. *J. Am. Chem. Soc.* **2001**, *123*, 8811–8824.

(24) Plavec, J.; Tong, W.; Chattopadhyaya, J. *J. Am. Chem. Soc.* **2001**, *115*, 9734–9746.

Scheme 1. Synthetic Pathways to Glycoligands **3**, **4** and Cu(II) Glycocomplexes **5**, **6**

122.9, 122.8, 120.4, 120.2, 113.0 (C_{O} isopropylidene), 105.6 (C1), 84.2 (C2), 77.9 (C4), 66.1 (C3), 48.5 (C5), 26.6 (CH_3), 26.1 ppm (CH_3); IR (KBr): $\nu = 3086$ ($\text{C}-\text{H}_{\text{ar}}$), 2988 ($\text{C}-\text{H}_{\text{ar}}$), (1603, 1571, 1549) ($\text{C}=\text{N}_{\text{Py}}$, $\text{C}=\text{N}_{\text{triazole}}$, $\text{C}=\text{C}$), 994 (Py), 893–710 ($\text{C}-\text{H}_{\text{ar}}$), 620 cm^{-1} (Py); HR-MS⁺: m/z [$\text{M} + \text{Na}$]⁺ calcd for $\text{C}_{22}\text{H}_{22}\text{N}_8\text{O}_3\text{Na}$, 469.1713; found, 469.1713; elemental analysis calcd (%) for $\text{C}_{22}\text{H}_{22}\text{N}_8\text{O}_3$: C, 59.18; H, 4.97; N, 25.1; found: C, 58.92; H, 4.87; N, 24.9.

3,5-Dideoxy-3,5-di(pyridin-2'-yl-1,2,3-triazol-1-yl)-1,2-O-isopropylidene- α -D-ribofuranose (4). $R_f = 0.14$ (DCM/EtOAc/MeOH 8.5:1:0.5); ¹H NMR (300 MHz, CDCl_3): $\delta = 8.56$ –8.59 (m, 2H, 2 \times H_{Py}), 8.42 (s, 1H, $\text{H}_{-\text{triazole}}$), 8.31 (s, 1H, $\text{H}_{-\text{triazole}}$), 8.17 (d, ³ $J(\text{H,H}) = 8.1$ Hz, 1H, H_{Py}), 8.12 (d, ³ $J(\text{H,H}) = 7.9$ Hz, 1H, H_{Py}), 7.79 (d, ³ $J(\text{H,H}) = 8.1$ Hz, 1H, H_{Py}), 7.74 (d, ³ $J(\text{H,H}) = 7.9$ Hz, 1H, H_{Py}), 7.19–7.28 (m, 2H, 2 \times H_{Py}), 5.94 (d, ³ $J(\text{H,H}) = 2.7$ Hz, 1H, H1), 5.00–5.04 (m, 1H), 4.79–4.90 (m, 4H), 1.60 (s, 3H, CH_3), 1.33 ppm (s, 3H, CH_3); ¹³C NMR (90 MHz, CDCl_3): $\delta = 150.0$, 149.9, 149.4, 149.3, 148.6, 148.5, 137.0, 136.9, 124.0, 123.1, 122.9, 122.5, 120.4, 120.3, 114.3 (C_{O} isopropylidene), 104.3 (C1), 78.6 (C3), 76.2 (C4), 62.2 (C2), 50.1 (C5), 26.6 (CH_3), 26.6 ppm (CH_3); IR (KBr): $\nu = 3143$ ($\text{C}-\text{H}_{\text{ar}}$); 2986 ($\text{C}-\text{H}_{\text{ar}}$); (1602, 1571, 1549) ($\text{C}=\text{N}_{\text{Py}}$, $\text{C}=\text{N}_{\text{triazole}}$, $\text{C}=\text{C}$); 994 (Py); 884–711 ($\text{C}-\text{H}_{\text{ar}}$); 620 cm^{-1} (Py); HR-MS⁺: m/z [$\text{M} + \text{Na}$]⁺ calcd for $\text{C}_{22}\text{H}_{22}\text{N}_8\text{O}_3\text{Na}$, 469.1713; found, 469.1727; elemental analysis calcd (%) for $\text{C}_{22}\text{H}_{22}\text{N}_8\text{O}_3 \cdot (11/20)\text{H}_2\text{O}$: C, 57.47; H, 5.07; N, 24.39; found: C, 57.47; H, 5.02; N, 24.28. Crystals suitable for diffraction were obtained by a slow evaporation of a dichloromethane solution of **4** (Table S4, Supporting Information).

Preparation of Compounds 5 and 6. Ligands **3** and **4** (50 mg) were dissolved in 1 mL of dichloromethane. An equimolar amount of $\text{Cu}(\text{NO}_3)_2 \cdot 3\text{H}_2\text{O}$ was dissolved separately in 1 mL absolute ethanol and 1 mL of water. The solutions were mixed, and an hyperchromic effect was observed. Crystals suitable for X-ray diffraction study were isolated after slow evaporation of the majority of the solvent for **3** but not for **4**. The complex formation, involving coordination of pyridine and triazole to Cu(II), was also evidenced by IR measurement: $\text{C}=\text{N}$ bond stretching frequencies of pyridine and triazole, and aromatic $\text{C}=\text{C}$ stretching was shifted from 1600, 1570, and 1549 cm^{-1} to 1630 (shoulder), 1620, and 1585 cm^{-1} .^{30–33} Ring breathing, in-plane bending, and out-of-plane bending vibrations of the pyridine ring occurring at 995 and 620 cm^{-1} are also appreciably

shifted to higher frequencies, viz., 1020 and 650 cm^{-1} in the spectra of complexes, indicating coordination through the ring nitrogen.³⁴

[Cu₂(3)₂(NO₃)₄·2H₂O, 5. Green crystals. Yield: quantitative. ES-MS m/z (intensity, %): 447.1 [**3** + H]⁺ (16); 469.0 [**3** + Na]⁺ (20); 509.0 [**3** + Cu]⁺ (52). HRMS-ES⁺ m/z : calcd for $\text{C}_{22}\text{H}_{22}\text{O}_3\text{N}_8\text{Cu}$, 509.1105; found 509.11162. HRMS-ES⁺ (in acetonitrile) m/z : calcd for $\text{C}_{22}\text{H}_{22}\text{O}_3\text{N}_8^{63}\text{Cu}$, 509.1111; found 509.1116. IR ν (cm^{-1}), selected bands: 3435 (O–H); 3109 ($\text{C}-\text{H}_{\text{ar}}$); (1630, 1620, 1584) ($\text{C}=\text{N}_{\text{Py}}$, $\text{C}=\text{N}_{\text{triazole}}$, $\text{C}=\text{C}_{\text{Py}}$); 1023 (Py); 649 (Py); elemental analysis calcd (%) for $\text{C}_{44}\text{H}_{44}\text{Cu}_2\text{N}_{16}\text{O}_8 \cdot 4\text{NO}_3 \cdot 10\text{H}_2\text{O}$: C, 36.49; H, 4.45; N, 19.34; found: C, 36.41; H, 4.23; N, 19.15.

6. Green precipitate. ES-MS m/z (intensity, %): 447.1 [**4** + H]⁺ (22); 469.0 [**4** + Na]⁺ (12); 508.9 [**4** + Cu]⁺ (58). HRMS-ES⁺ (in water) m/z : calcd for $\text{C}_{22}\text{H}_{22}\text{O}_3\text{N}_8\text{Cu}$, 509.1105; found 509.11011. HRMS-ES⁺ (in acetonitrile) m/z : calcd for $\text{C}_{22}\text{H}_{22}\text{O}_3\text{N}_8^{63}\text{Cu}$, 509.1111; found 509.1129. IR ν (cm^{-1}), selected bands: 3428 (O–H); 3110 ($\text{C}-\text{H}_{\text{ar}}$); (1630, 1621, 1587) ($\text{C}=\text{N}_{\text{Py}}$, $\text{C}=\text{N}_{\text{triazole}}$, $\text{C}=\text{C}$); 1024 (Py); 649 (Py).

Crystallographic Studies. Details of the crystal data, data collection and refinement are given in Tables S2 and S4, Supporting Information. The diffraction intensities of crystals were collected with graphite-monochromatized Mo K α radiation. Data collection and cell refinement were carried out using a Bruker Kappa X8 APEX II diffractometer. The temperature of the crystal was maintained at the selected value (100K) by means of a 700 series Cryostream cooling device to within an accuracy of ± 1 K. Intensity data were corrected for Lorentz polarization and absorption factors. The structures were solved by direct methods using SHELXS-97, and refined against F^2 by full-matrix least-squares methods using SHELXL-97 with anisotropic displacement parameters for all nonhydrogen atoms. All calculations were performed by using the crystal structure crystallographic software package WINGX. The structure was drawn using ORTEP3. Hydrogen atoms were located on a difference Fourier map and introduced into the calculations as a riding model with isotropic thermal parameters. At the end of the least-squares refinement of **5**, the density maps show that there is no residual density greater than 0.18 $\text{e}/\text{Å}^3$ in the cavity between the two copper atoms. This indicates without any ambiguity the absence of any solvent molecule in between the two copper ions.

Results and Discussions

Synthesis. The two ligands **3** and **4** are based on conformationally constrained bicyclic *xylo*- and *ribo*-1,2-*O*-isopropylidene-furano scaffolds and differ only by the absolute

(30) Alves, W. A.; De Almeida Santos, R. H.; Paduan-Filho, A.; Becerra, C. C.; Birun, A. C.; da Costa Ferreira *Inorg. Chim. Acta* **2004**, *357*, 2269–2278.

(31) Zaydoun, S.; Saidi Idrissi, M.; Garrigou-Lagrange, C. *Can. J. Chem.* **1987**, *65*, 2509–2512.

(32) Ouïjja, N.; Guédira, F.; Zaydoun, S.; Aouial, M.; Saidi Idrissi, M.; Lautié, A. *J. Chim. Phys.* **1999**, *96*, 934–946.

(33) Sarkar, B.; Bocelli, G.; Cantoni, A.; Ghosh, A. *Polyhedron* **2008**, *693*–700.

(34) Hartmann, J. A. R.; Kammier, A. L.; Spracklin, R. J.; Pearson, W. H.; Combariza, M. Y.; Vachet, R. W. *Inorg. Chim. Acta* **2004**, *357*, 1141–1151.

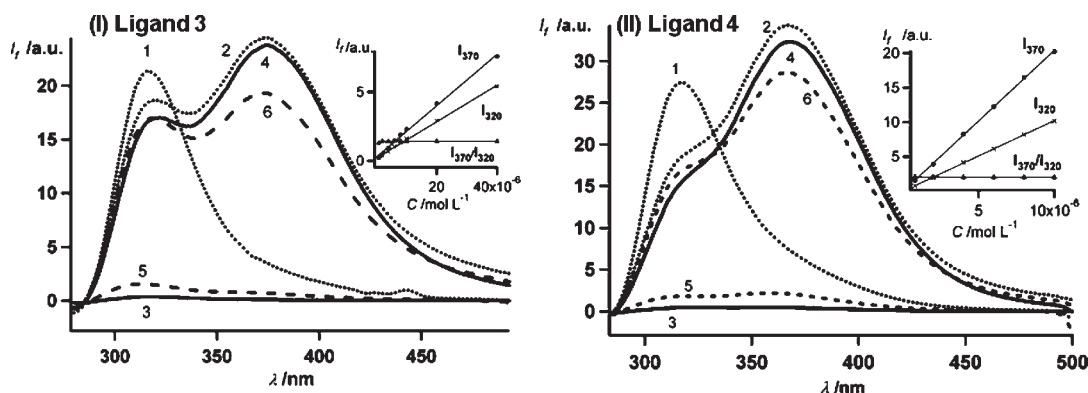


Figure 1. (I) Fluorescence emission spectra of **3**. (II) Fluorescence emission spectra of **4**; $c = 8 \times 10^{-6} \text{ mol L}^{-1}$ in [1] EtOH, [2] EtOH/H₂O (15:85), [3] DMSO, [4] DMSO/H₂O (15:85), [5] AcN (CH₃CN), and [6] AcN/H₂O (15:85). $\lambda_{\text{exc}} = 260 \text{ nm}$; the spectra are corrected from the O.D. at $\lambda_{\text{exc}} = 260 \text{ nm}$. Inset: intensity of the bands at 320 and 370 nm (DMSO/H₂O 15:85) from 8×10^{-7} to 4×10^{-5} (I) or $1 \times 10^{-5} \text{ mol L}^{-1}$ (II).

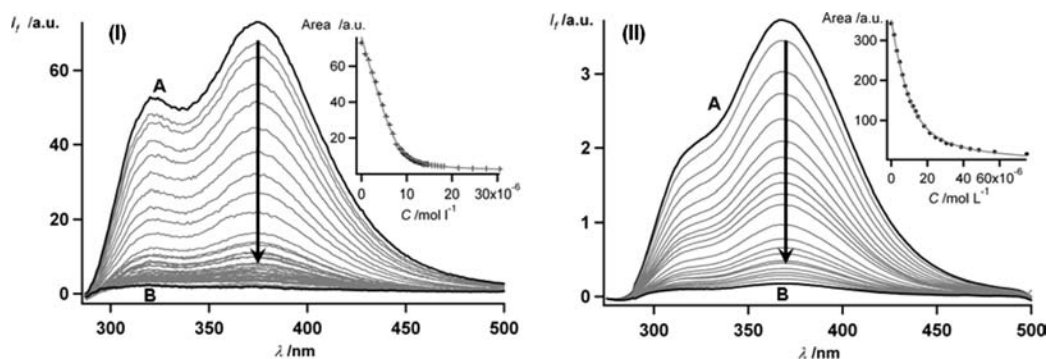


Figure 2. (I) Fluorescence spectra obtained for the titration of **3**, (II) Fluorescence spectra obtained for the titration of **4** in DMSO:H₂O (15:85) ($c = 8 \times 10^{-6} \text{ mol L}^{-1}$) with Cu(ClO₄)₂ [(I) from 0 (A) to 15 equiv; (B), (II) from 0 (A) to 4.5 equiv (B)]. $\lambda_{\text{exc}} = 260 \text{ nm}$. Inset: titration curve of the normalized integrated fluorescence as a function of Cu(II) concentration.

configuration of the C3 atom. They were prepared from 3,5-diazo-3,5-dideoxy-1,2-*O*-isopropylidene- α -D-pentofuranoses **1** and **2** by using the Huisgen 1,3-dipolar cycloaddition.³⁵

Treatment of **1** or **2** in a 1:1 *t*-BuOH/H₂O mixture with 2-ethynylpyridine in presence of Cu(I) (CuSO₄ and sodium ascorbate) to catalyze the [2 + 3] cycloaddition gave the expected compounds **3** and **4** in 91% and 62% yield, respectively (Scheme 1).

Solvatochromism and Titration by Fluorescence. Fluorescence emission spectra of **3** and **4** were recorded in ethanol, DMSO, and acetonitrile (Figure 1). They exhibit solvatochromism, with quenching of fluorescence in DMSO, acetonitrile but not in ethanol (emission at 320 nm). The addition of 85% water induced the apparition of a second emission band at ca. 370 nm with an increase in the fluorescence intensity (Figure 1 and Table S1, Supporting Information). It was assigned to the formation of excimers by π -stacking due to hydrophobic interaction. The ratio of the two bands is independent of the concentration (Figure 1, insets), indicating that the π -stacking is intramolecular. Indeed, the disubstitution on a unique monosaccharide platform induces a proximity of the claws and allows an intramolecular organization of the ligand through hydrophobic interaction.

Upon coordination to Cu(II), the fluorescence is quenched. A titration experiment was therefore carried out by

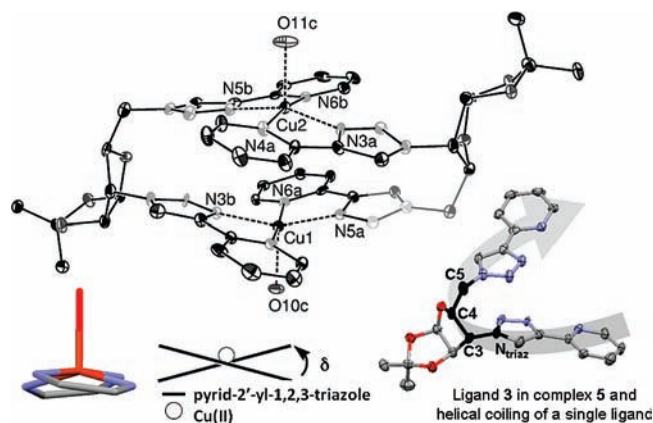


Figure 3. Crystal structure of the cationic moiety of **5**. Hydrogen atoms are not shown for clarity. Displacement ellipsoids at the 30% probability level. Insets: schematic view of the δ skew conformation and of the left-handed (*M*)³ helical coiling up of a single ligand. In black: the N_{triazole}–C3–C4–C5 dihedral angle of one ligand **3** in complex **5**.

fluorescence; by the addition of successive equivalents of Cu(II), the fluorescence intensity progressively decreased (Figure 2). The binding ratio of **3** and **4** with Cu(II) was established to be 1:1 (L:M), and the dissociation constants of both ligands were $(0.40 \pm 0.01) \times 10^{-6}$ and $(4.0 \pm 0.1) \times 10^{-6}$, respectively, by using a well-fitted titration curve with a 1:1 complexation equation model (Figure 2, insets).

Description of the Crystal Structure. Crystals of **5** suitable for X-ray diffraction could be obtained by slow

(35) Kolb, H. C.; Finn, M. G.; Sharpless, K. B. *Angew. Chem., Int. Ed.* **2001**, *40*, 2004–2021.

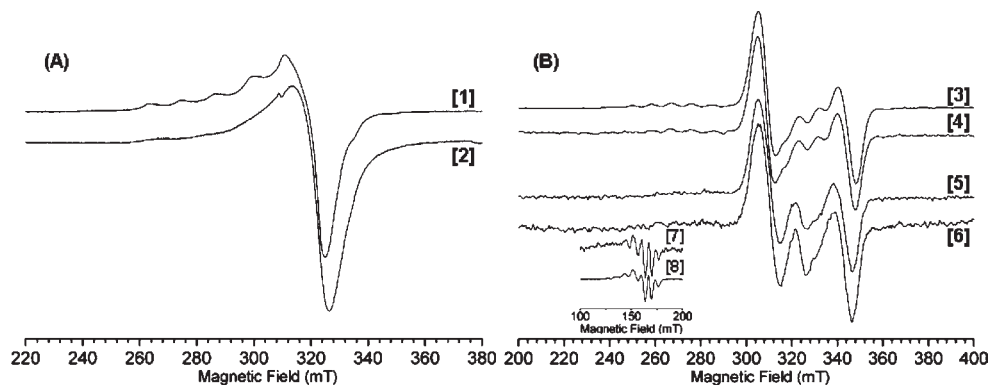


Figure 4. (A) 9.4 GHz EPR spectra in toluene/acetone/DMSO (3:3:4), $c = 10^{-3} \text{ mol L}^{-1}$, $T = 5 \text{ K}$, mod. amp. 0.5 mT, microwave power $0.8 \mu\text{W}$: [1] **6** and [2] **5**; $T = 5 \text{ K}$, mod. amp. 0.5 mT, microwave power $0.8 \mu\text{W}$; (B) 9.4 GHz EPR spectra in H_2O /glycerol [3] **5**, $c = 10^{-2} \text{ mol L}^{-1}$, $T = 10 \text{ K}$, mod. amp. 0.5 mT, microwave power $8.0 \mu\text{W}$, [4] **5**, $c = 10^{-4} \text{ mol L}^{-1}$, $T = 10 \text{ K}$, mod. amp. 1.5 mT, microwave power $8.0 \mu\text{W}$, [5] **6**, $c = 10^{-3} \text{ mol L}^{-1}$, $T = 10 \text{ K}$, mod. amp. 1 mT, microwave power 0.50 mW, [6] **6**, $c = 10^{-4} \text{ mol L}^{-1}$, $T = 10 \text{ K}$, mod. amp. 0.5 mT, microwave power 0.13 mW , [7] **5**, $c = 10^{-2} \text{ mol L}^{-1}$, $T = 10 \text{ K}$, mod. amp. 0.5 mT, microwave power $8.0 \mu\text{W}$, [8] **6**, $c = 10^{-3} \text{ mol L}^{-1}$, $T = 10 \text{ K}$, mod. amp. 1 mT, microwave power 16 mW . Arbitrary units for intensities for each spectrum.

evaporation of a solution of equimolar amounts of $\text{Cu}(\text{NO}_3)_2 \cdot 3\text{H}_2\text{O}$ and **3** in $\text{CH}_2\text{Cl}_2/\text{MeOH}/\text{H}_2\text{O}$ 1:1:1 (Scheme 1). The structure of the complex **5** (Figure 3) is dimeric, with triazole involved in the coordination as in a few examples in the literature.^{29,36–38,23}

The two $\text{Cu}(\text{II})$ ions are coordinated to four nitrogen atoms from two different ligands. The coordination sphere of each $\text{Cu}(\text{II})$ cation is a distorted square pyramid, with water molecules in apical positions (O11c and O10c) and a τ factor³⁹ of 0.27 (Cu1) and 0.22 (Cu2) ($\tau = 0$ for a square pyramid, and $\tau = 1$ for a trigonal bipyramid). The Cu–Cu separation within the dimer was found to be $3.950(1) \text{ \AA}$ without any bridging molecule. This absence of any bridging ligand in the solid state was confirmed by the behavior of the magnetic susceptibility as a function of T , which indicates no antiferromagnetic coupling (Figure S2, Supporting Information). Strong π – π interaction between the two triazolyl-pyridyl claws—aromatic centroids separation smaller than 3.49 (triazole) and 3.65 \AA (pyridine)⁴⁰—are most likely responsible for the intramolecular excimer signals observed in aqueous media. Each ligand is coiling up around the Cu–Cu axis with a left-handed helicity, and the two copper ions show a δ chirality in the skew line reference system.⁴¹ The orientation of the pyridyl-triazolyl claw bound to C3 is determined both by the stereochemistry at the C3, that is by the dihedral angle $\text{N}_{\text{triazole}}\text{—C3—C4—C5}$ (Figure 3, in black) and by strong stabilizing π – π interactions that are also controlling the orientation of the claw connected at C5 (Figure 3,

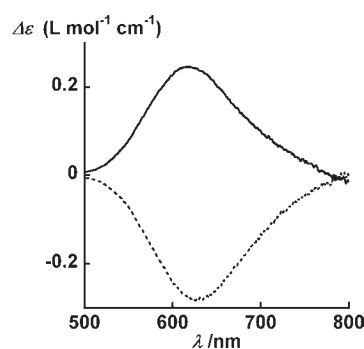


Figure 5. CD spectra in H_2O ($c = 10^{-2} \text{ mol L}^{-1}$) of the complexes **5** (—) and **6** (---).

insets). This feature determines the overall coiling up around the Cu–Cu axis. Similar discrete $\text{Cu}(\text{II})$ double-deck complexes are rather rare in the literature.^{42–44} Interestingly, the π -stacking is stabilizing the double-deck structure of the chelating rigid claws, preventing their chelation to a unique metal center. In the case of glycoligands built on the same central scaffolds but with more flexible appended Lewis bases (*O*-2-picoline and *N,N*-di-2-picoline),¹⁸ no such π -stacking was stabilizing any double-deck of the chelating claws, and the $\text{Cu}(\text{II})$ complexes were obtained as monometallic.¹⁸

EPR Measurements. In order to investigate the environment of $\text{Cu}(\text{II})$ ions in solution, EPR studies were carried out using equimolar mixture of **3** (or **4**) and $\text{Cu}(\text{II})$ in toluene/acetone/DMSO 3:3:4. As shown in Figure 4A, under these conditions, a signal characteristic of a $\text{Cu}(\text{II})$ $S = 1/2$ in a distorted square-planar environment was observed in organic solvent with the corresponding parameters $g_{\parallel} = 2.3$, $A_{\parallel} \approx 560 \text{ MHz}$, and $g_{\perp} = 2.09$ for **3** and $g_{\parallel} = 2.4$, $A_{\parallel} \approx 410 \text{ MHz}$, and $g_{\perp} = 2.09$ for **4**, estimated by direct measurements on the spectra.⁴⁵ The spectra show, therefore, similar characteristics. By contrast, in

(36) Colasson, B.; Save, M.; Milko, P.; Roithova, J.; Schroder, D.; Reinaud, O. *Org. Lett.* **2007**, *9*, 4987–4990.

(37) Mindt, T. L.; Struthers, H.; Brans, L.; Anguelov, T.; Schweinsberg, C.; Maes, V.; Tourwe, D.; Schibli, R. *J. Am. Chem. Soc.* **2006**, *128*, 15096–15097.

(38) Monkowius, U.; Ritter, S.; König, B.; Zabel, M.; Yersin, H. *Eur. J. Inorg. Chem.* **2007**, 4597–4606.

(39) Addison, A. W.; Rao, T. N.; Reedjick, J.; Rijn, V.; Verschoor, G. C. *J. Chem. Soc., Dalton Trans.* **1984**, 1349–1356.

(40) π – π -stacking: the stacking between the pyridines containing N4a/N4b and N6a/N6b is characterized by a slip angle of 4.91° and 4.83° and a centroid separation of 3.604 and 3.642 \AA , respectively. Similarly, a smaller interaction between the triazolyl containing N3a/N5a (respectively N3b/N5b) is characterized by a slip angle of 15.07° (respectively 14.87°) and a centroid separation of 3.486 \AA (respectively 3.458 \AA).

(41) Von Zelewsky, A. *Stereochemistry of coordination compounds*; Wiley: Chichester, U.K., 1996.

(42) Kim, K. M.; Kam, K.; Kang, T. Y.; Park, J. S.; Song, R.; Jun, M. *Chem. Commun.* **2003**, 1410–1411.

(43) Barbour, L. J.; Orr, G. W.; Atwood, J. L. *Nature* **1998**, *393*, 671–673.

(44) Kim, K. M.; Park, J. S.; Kim, Y.; Jun, Y. J.; Kang, T. Y.; Sohn, Y. S.; Jun, M. *Angew. Chem., Int. Ed.* **2001**, *40*, 2458–2460.

(45) A_{\parallel} has been estimated from the spacing of the first two hyperfine lines.

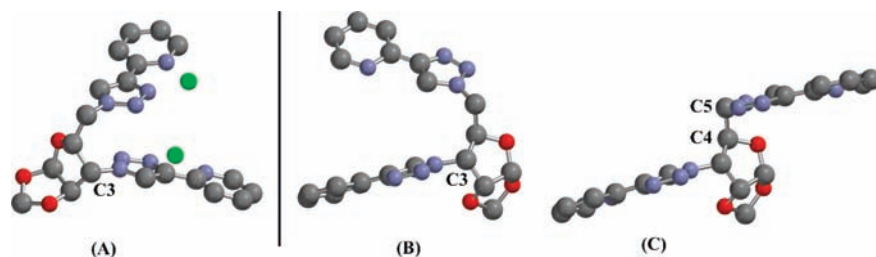


Figure 6. (A) View of ligand **3** in the structure of **5**. (B) View of the conformation of **4** obtained by a 180° rotation around the C4–C5 bond. (C) structure of ligand **4**.⁵²

water, the EPR spectrum is dominated by a signal characteristic of a $S = 1$ system for strongly coupled homovalent Cu(II) dimers (Figure 4B), with a half-field transition at $g \sim 4$ due to the triplet–triplet transition ($\Delta M_s = 2$) (see inset of Figure 4B). This indicates that water^{46,47} is able to bridge two Cu(II) ions.^{48,49} No change in the EPR spectra was observed upon dilution (10^{-2} to 10^{-4} mol L⁻¹), the signal being scaled by a factor corresponding to the dilution. This result is in favor of an intramolecular dimer, with the bridging water inside the cavity. In the organic solvent, due to the fact that toluene may interfere with the π -stacking properties of the ligand, we have also performed the EPR measurements in an acetonitrile/DMSO mixture and obtained similar results (Figure S6, Supporting Information).

UV–vis Measurements. The electronic properties of **5** and **6** were also studied by UV–vis spectroscopy. Similar UV–vis spectra in a toluene/acetone/DMSO (3:3:4) solution were recorded for both **5** and **6** with a broad d–d band at, respectively, 742 ($\epsilon = 56$ L mol⁻¹ cm⁻¹) and 768 nm ($\epsilon = 46$ L mol⁻¹ cm⁻¹) (Figure S7, Supporting Information). Upon addition of water to this organic solution, the d–d band is shifted toward higher energy, and a shoulder at ca. 370 nm appears (Figure S7, Supporting Information). In water, UV–vis spectra of **5** and **6** exhibit d–d bands at, respectively, 657 ($\epsilon = 66$ L mol⁻¹ cm⁻¹) and 673 nm ($\epsilon = 63$ L mol⁻¹ cm⁻¹) (Figure S7, Supporting Information) and a band at ca. 370 nm (Figure S7, Supporting Information), assigned to the O–Cu ligand–metal charge transfer of the bridging water molecule between the two Cu(II) ions in the dimeric structure. The observed d–d bands are indicative of a distorted tetragonal pyramidal environment, which is in adequation with the X-ray analysis in the solid state. UV–vis spectra in organic solution and in water are consistent with EPR spectra in the same solutions. Finally, the complexes **5** and **6** display bands in the usual range for Cu(II) dimeric species.^{30,50}

Circular Dichroism Measurements. The CD spectra of solutions of **5** and **6** were recorded in water in the region of

Cu(II) d–d transitions, showing a mirror-image pattern typical of enantiomers (Figure 5). The very small differences in absorption spectra (Figure S7, Supporting Information), CVs (Figure S3, Supporting Information), EPR (Figure 4 and Figure S6, Supporting Information), dissociation constants (see above) in water indicate small local variations between the structure of **5** and **6** at the metal site. This is probably due to differences in the constraints imposed by the two scaffolds on the coordination sphere. The most striking feature is the mirror-image CD pattern (Figure 5). This indicates that the Cu(II) centers in **5** and **6** are in a very similar environment with a pseudoenantiomer coordination sphere.

In order to understand this result, a suitable conformation of **4**, successfully crystallized for X-ray analysis (Table S4, Supporting Information), was sought for. On Figure 6 is shown the structure of ligand **3** in complex **5** (Figure 6A) and ligand **4** (Figure 6C). By a rotation around the C5–C4 bond in **4**, it was possible to find a conformation of **4** offering a coiling of the claws opposite to that in **5** (Figure 6B). The opposite pseudoenantiomeric character at the metal center can be understood as an opposite coiling induced by the only difference existing between the ligands, that is by the dihedral angle $N_{\text{triazole}}\text{–C3–C4–C5}$. It suggests that this difference in the central structure, combined with rigid aromatic chelates, is able to induce a predetermination of stereochemistry at the metal center, as defined by Knof et von Zelewsky:⁵¹ “We speak of predetermination of chirality at a metal center if one of the two species is preferentially formed in a (diastereoselective) synthesis of a metal complex.” The ribo/xylo central structure, combined to rigid aromatic chelating groups, in glycoligands **3** and **4** is able to induce a predetermination⁵¹ of stereochemistry at the metal center by the ligand.¹⁸

Conclusion

This article presents an original control of the structure in coordination Cu(II) complexes. The results indicate that the glycoligands **3** and **4** based on the conformationally restrained *xylo*- and *ribo*-furano scaffolds are preorganized in water through π – π stacking due to hydrophobic interaction, as evidenced by excimer observation. The combination of π -stacking and chiral backbone leads to chiral dimeric copper complexes, with an original helical coiling of two ligands around the Cu–Cu axis, as shown by the structure of **5**.

(51) Knof, U.; von Zelewsky, A. *Angew. Chem., Int. Ed.* **1999**, *38*, 302–322.

(52) It should be noted that in the structure of **4**, the nitrogen atoms of pyridine and triazole in the same claw do not point in the same direction, which would simply require a 180° rotation.

(46) Water molecule refers here to any protonated state of water (H₂O, HO⁺, or O₂⁺). The most probable state is here H₂O or hydroxo: the pH of the EPR water/glycerol solution was measured to be 5 (biotrod microelectrode Metrohm), and the acido-basic couple [Cu(H₂O)₄]²⁺/[Cu(H₂O)₃(OH)]⁺ has been reported to have a pK_a of 7.3.

(47) Sillen, L. G.; Martell, A. E. *Stability constants of metal ion complexes*; Royal Society of Chemistry: London, 1971.

(48) Thompson, L. K.; Mandal, S. K.; Gabe, E. J.; Lee, F. L.; Addison, A. W. *Inorg. Chem.* **1987**, *26*, 657–664.

(49) Dubler, E.; Hänggi, G.; Schmalle, H. *Inorg. Chem.* **1990**, *29*, 2518–2523.

(50) Stachova, P.; Valigura, D.; Koman, M.; Melnik, M.; Korabik, M.; Mrozinski, J.; Glowiak, T. *Polyhedron* **2004**, *23*, 1303–1308.

Compound **6**, prepared from the epimeric ligand **4** shows a mirror-image circular dichroism (CD) spectrum in the d–d region of the Cu(II). Interestingly, these two diastereoisomer ligands lead to pseudoenantiomers Cu(II) complexes. There is, as defined by von Zelewski, a predetermination of chirality. The rigidity of the claw and the disubstitution on a unique monosaccharide platform inducing a chelate effect and π -stacking here are of importance. In the structure of **5**, which is an unusual double-deck type structure with π – π interaction between the triazolyl-pyridyl chelating claws, defines a small cavity between the two Cu(II) ions that is suggested to be able to host a bridging water molecule. These results show the interest of glycoligands to finely tune the chelation site structure, with preorganization for the dimeric

chelation of Cu (II), control of the nuclearity and predetermination of stereochemistry by the combination of π -stacking and chiral backbone.

Acknowledgment. Financial support was provided by the French Government: ACI “Jeune Chercheur” 2004-J4044 (C.P.).

Supporting Information Available: UV–vis spectra and quantum yield of the ligands. Crystal data and structure refinement for **4** and **5**. Magnetic measurement for **5**. Cyclic voltammetry of the complexes **5** and **6**. Fluorescence for **4**. This material is available free of charge via the Internet at <http://pubs.acs.org>.